



Article

Two New Phenolic Glycosides with Lactone Structural Units from Leaves of *Ardisia crenata* Sims with Antibacterial and Anti-Inflammatory Activities

 Huihui Tao , Yongqiang Zhou *, Xin Yin , Xin Wei and Ying Zhou *

College of Pharmacy, Guizhou University of Traditional Chinese Medicine, Guiyang 550025, China; thlc922@163.com (H.T.); yinxin110901@163.com (X.Y.); sfweixin@163.com (X.W.)

* Correspondence: zhouxiaoqiang1988@126.com (Y.Z.); yingzhou71@sina.com (Y.Z.); Tel.: +86-0851-8830-8059 (Y.Z.); +86-0851-8823-3090 (Y.Z.)

Abstract: Two new lactones, named Ardisicreolides A–B (1–2), together with four known flavonoids, Quercetin (3), Myricetrin (4), Quercitrin (5), Tamarixetin 3-O-rhamnoside (6), were isolated from the ethyl acetate portion of 70% ethanol extracts of dried leaves from *Ardisia crenata* Sims. These compounds were identified from *Ardisia crenata* Sims for the first time. The structures of 1–6 were elucidated according to 1D and 2D-NMR methods and together with the published literature. All of the isolated compounds were evaluated for in vitro anti-microbial effect against *Escherichia coli*, *Pseudomonas aeruginosa*, *Enterococcus faecalis*, *Proteus vulgaris*, *Staphylococcus aureus*, and *Bacillus subtilis*. In addition, compounds 1–2 were assessed for anti-inflammatory activity by acting on LPS-induced RAW 264.7 macrophage cells in vitro. The results showed that only compound 2 exhibited moderate antibacterial activity on *Bacillus subtilis*. Moreover, compounds 1 and 2 were found to significantly inhibit the production of nitric oxide (NO) and reduce the release of tumor necrosis factor- α (TNF- α), interleukin-1 β (IL-1 β), interleukin-4 (IL-4), and interleukin-10 (IL-10) in LPS-induced RAW 264.7 macrophage cells. The present data suggest that lactones from the leaves of *A. crenata* Sims might be used as a potential source of natural anti-inflammatory agents.

Keywords: *Ardisia crenata* Sims; lactone; antibacterial; anti-inflammatory; natural product



Citation: Tao, H.; Zhou, Y.; Yin, X.; Wei, X.; Zhou, Y. Two New Phenolic Glycosides with Lactone Structural Units from Leaves of *Ardisia crenata* Sims with Antibacterial and Anti-Inflammatory Activities.

Molecules **2022**, *27*, 4903. <https://doi.org/10.3390/molecules27154903>

Academic Editors: Gui-Guang Cheng, Lu Liu and Tao Feng

Received: 11 July 2022

Accepted: 29 July 2022

Published: 31 July 2022

Publisher's Note: MDPI stays neutral with regard to jurisdictional claims in published maps and institutional affiliations.



Copyright: © 2022 by the authors. Licensee MDPI, Basel, Switzerland. This article is an open access article distributed under the terms and conditions of the Creative Commons Attribution (CC BY) license (<https://creativecommons.org/licenses/by/4.0/>).

1. Introduction

There are about 500 species of plants in the genus *Ardisia*, which are widely distributed in subtropical and tropical regions [1,2]. The *Ardisia crenata* Sims is a common evergreen shrub belonging to *Ardisia* of Myrsinaceae with red fruits at maturity [3]. In China, the roots of the red-fruited *A. crenata* Sims are used as a traditional Chinese medicine “Zhushagen” [4], which is widely used for the treatment of respiratory infections, toothache, arthralgia, menstrual problems, and fertility regulation [5–7]. These pharmacological activities are often closely related with different kinds of chemical constituents from the roots of *A. crenata* Sims. Previous phytochemical studies on the roots of *A. crenata* Sims have mainly revealed active constituents including triterpenoid saponins, coumarins, phytosterols, and benzoquinones [8–10]. Recently, researchers have extensively investigated these compounds for their anti-tumor, immunosuppressive, anti-inflammatory, and antimicrobial activities [11–15].

The existing studies have rarely identified lactones, which often have better pharmacological activities including anti-inflammatory activities [16–18]. Such constituents are mainly obtained through chemical synthesis or microbial biosynthesis, which involve many pathways and enzymes [19,20]. Previous studies on *A. crenata* Sims have focused on the root of *A. crenata* Sims, however, the non-medicinal parts of *A. crenata* Sims have been less studied. In this report, in order to expand the available resources and search for new bioactive constituents of *A. crenata* Sims, we described the isolation and structural elucidation

of lactones and flavonoids. Moreover, the antibacterial and anti-inflammatory activities of two new lactones are discussed by the paper diffusion method and enzyme-linked immunosorbent (ELISA) assay.

2. Results and Discussion

2.1. Structure Elucidation

Compound **1** was separated as a light yellow amorphous solid. The molecular formula was inferred as $C_{26}H_{28}O_{11}$ according to the HR-ESI-MS analysis of m/z 539.1522 $[M + Na]^+$ (calculated value 539.1524 $[M + Na]^+$), and the calculated unsaturation (Ω) = 13. The 1H -NMR spectrum of compound **1** (Table 1) showed two aromatic ring proton signals δ_H 7.49 (2H, dd, $J = 1.9, 7.8$ Hz, H-2''', H-6'''); 7.26 (3H, *m*, H-3''', H-4''', H-5'''); δ_H 6.25 (1H, *d*, $J = 2.9$ Hz, H-3'); 6.19 (1H, *d*, $J = 2.9$ Hz, H-5'), a double bond signal δ_H 7.06 (1H, *d*, $J = 12.6$ Hz, H-7'''); 5.98 (1H, *d*, $J = 12.6$ Hz, H-8''') identified as *cis* by the coupling constant, together with one anomeric proton at δ_H 4.44 (1H, *d*, $J = 7.6$ Hz, H-1''). ^{13}C -NMR spectrum data (Table 1) revealed two benzene ring carbons and one pair of olefin carbons δ_C 103.4, 109.2, 120.3, 129.1, 130.0, 130.7, 133.0, 136.4, 138.5, 144.8, 151.5, 155.9, two ester carbonyl data δ_C 167.6, 180.5, and one sugar unit δ_C 64.5, 71.3, 75.4, 75.9, 77.9, 107.5, and the remaining four carbons were identified by DEPT 135° as three methylene δ_C 28.3, 29.5, 82.8 and one hypomethyl δ_C 36.5. Thus, the skeleton was identified as a five-membered lactone ring fragment by the key 1H - 1H COSY signal (Figure 1). The connection of each fragment was determined by key HMBC signals (Figure 1) including H₂-3 and H₁-5 to C-2; H₂-6 to C-4, C-1', C-5' and C-6'; H₁-6'' to C-5'', C-4' and C-9'''; H₁-8''' to C-9'''; H₁-7''' to C-2''' and C-9'''. The spectroscopic data of compounds **1** (Figures S2–S11) were available as Supporting Information. The structures are shown in Figure 2. The structure of compound **1** was similar to that of Myrsinoside A [21], differing in the cinnamoyl and pentadactyl lactone ring portions.

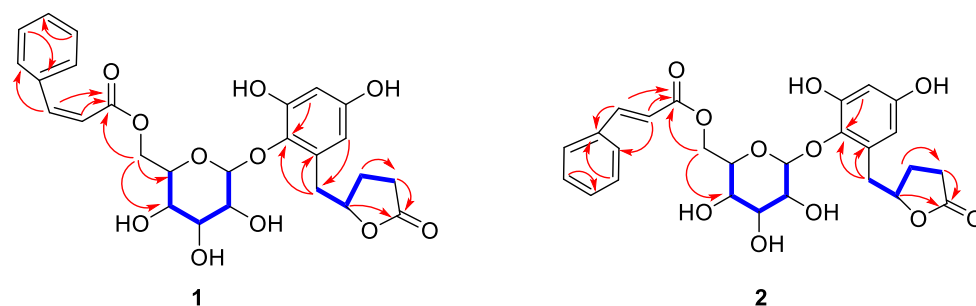
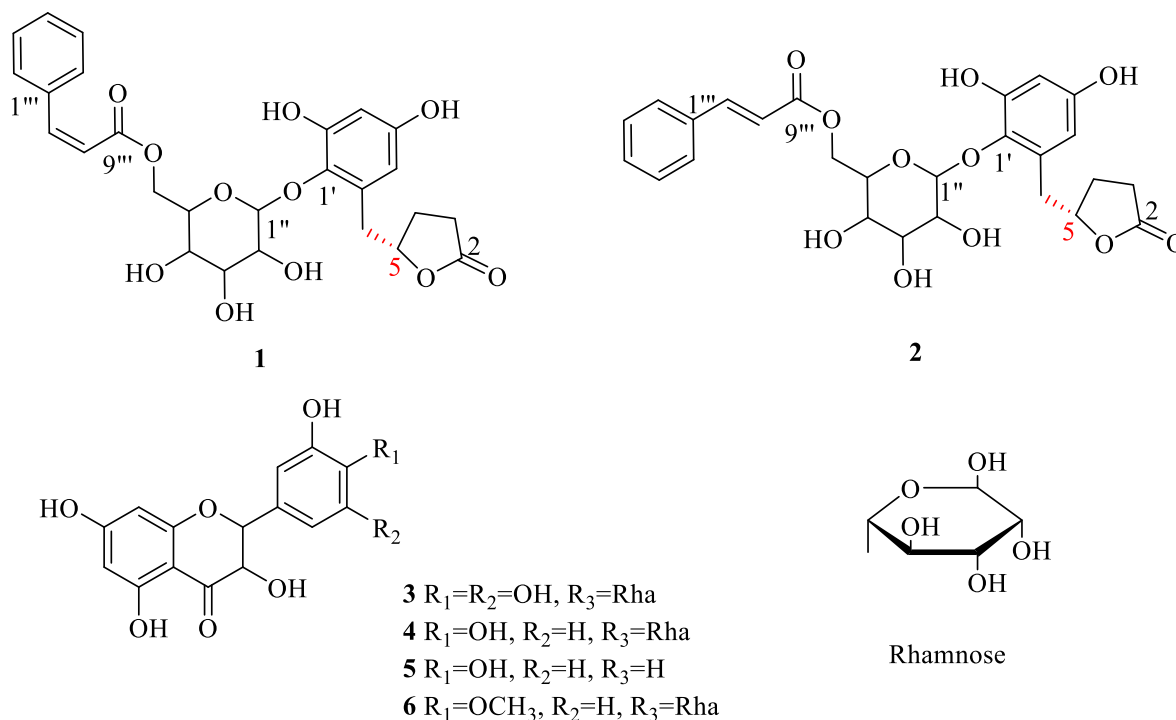


Figure 1. The key HMBC (H→C) and 1H - 1H COSY correlations of compounds **1**–**2**.

Acid hydrolysis of **1** provided D-glucose. In addition, the coupling constant of H₂-1'', $J = 7.6$ Hz indicated the configuration of the hydroxyl group at the anomeric carbon in sugar to be β . To further elucidate its absolute configuration, a combined CD spectrum with the electronic circular dichroism (ECD) spectrum of **1** recorded in MeOH showed a negative cotton effect at 208 nm, a positive cotton effect at 250 nm, a negative cotton effect at 267 to 296 nm, and a positive cotton effect at 297 to 325, which was broadly consistent with the calculated ECD data of the (5S) model (Figure 3). The calculation process could be found in the supporting information (Figure S1 and Tables S1–S3). Thus, the structure of **1** was established as ((2R,3S,4S,5R,6S)-6-(2,4-dihydroxy-6-(((S)-5-oxotetrahydrofuran-2-yl)methyl)phenoxy)-3,4,5-trihydroxytetrahydro-2H-pyran-2-yl)methyl (Z)-3-phenylacrylate and was named Ardisicreolides A (Figure 1).

Table 1. The ^1H and ^{13}C -NMR data of compounds 1–2 in CD_3OD (δ in ppm).

Position	Ardisicreolide A			Ardisicreolide B		
	δ_{C}	δ_{H}	(J in Hz)	δ_{C}	δ_{H}	(J in Hz)
2	180.5	-	-	180.4	-	-
3	29.5	2.35	m	29.5	2.45	dd (7.5, 8.9)
4	28.3	1.90, 2.19	m, m	28.3	1.96, 2.23	dtd (7.0, 8.9, 12.5), m
5	82.8	4.76	m	82.8	4.84	M
6	36.5	2.85, 3.15	dd (4.7, 14.1), dd (8.0, 14.1)	36.6	2.87, 3.25	dd (5.2, 14.0), dd (7.6, 14.0)
1'	138.5	-	-	138.6	-	-
2'	151.5	-	-	151.6	-	-
3'	103.4	6.25	d (2.9)	103.4	6.23	d (2.9)
4'	155.9	-	-	155.9	-	-
5'	109.2	6.19	d (2.9)	109.2	6.18	d (2.9)
6'	133.0	-	-	132.9	-	-
1''	107.5	4.44	d (7.6)	107.6	4.57	d (7.6)
2''	75.4	-	-	75.4	-	-
3''	77.9	-	-	77.9	-	-
4''	71.3	3.28~3.46	m (4H)	71.5	3.37~3.62	m (4H)
5''	75.9	-	-	76.0	-	-
6''	64.5	4.24, 4.50	dd (6.5, 12.0), dd (2.0, 12.0)	64.7	4.34, 4.59	dd (6.5, 12.0), dd (2.0, 12.0)
1'''	136.4	-	-	135.7	-	-
2''' 6'''	130.7	7.49	dd (1.9, 7.8, 2H)	130.1	7.61	dd (1.9, 7.8, 2H)
3''' 5'''	129.1	-	-	129.4	-	-
4'''	130.0	7.26	m (3H)	131.6	7.42	m (3H)
7'''	144.8	7.06	d (12.6)	146.8	7.73	d (16.0)
8'''	120.3	5.98	d (12.6)	118.5	6.54	d (16.0)
9'''	167.6	-	-	168.3	-	-

**Figure 2.** The structures of compounds 1–6 from the leaves of *A. crenata* Sims.

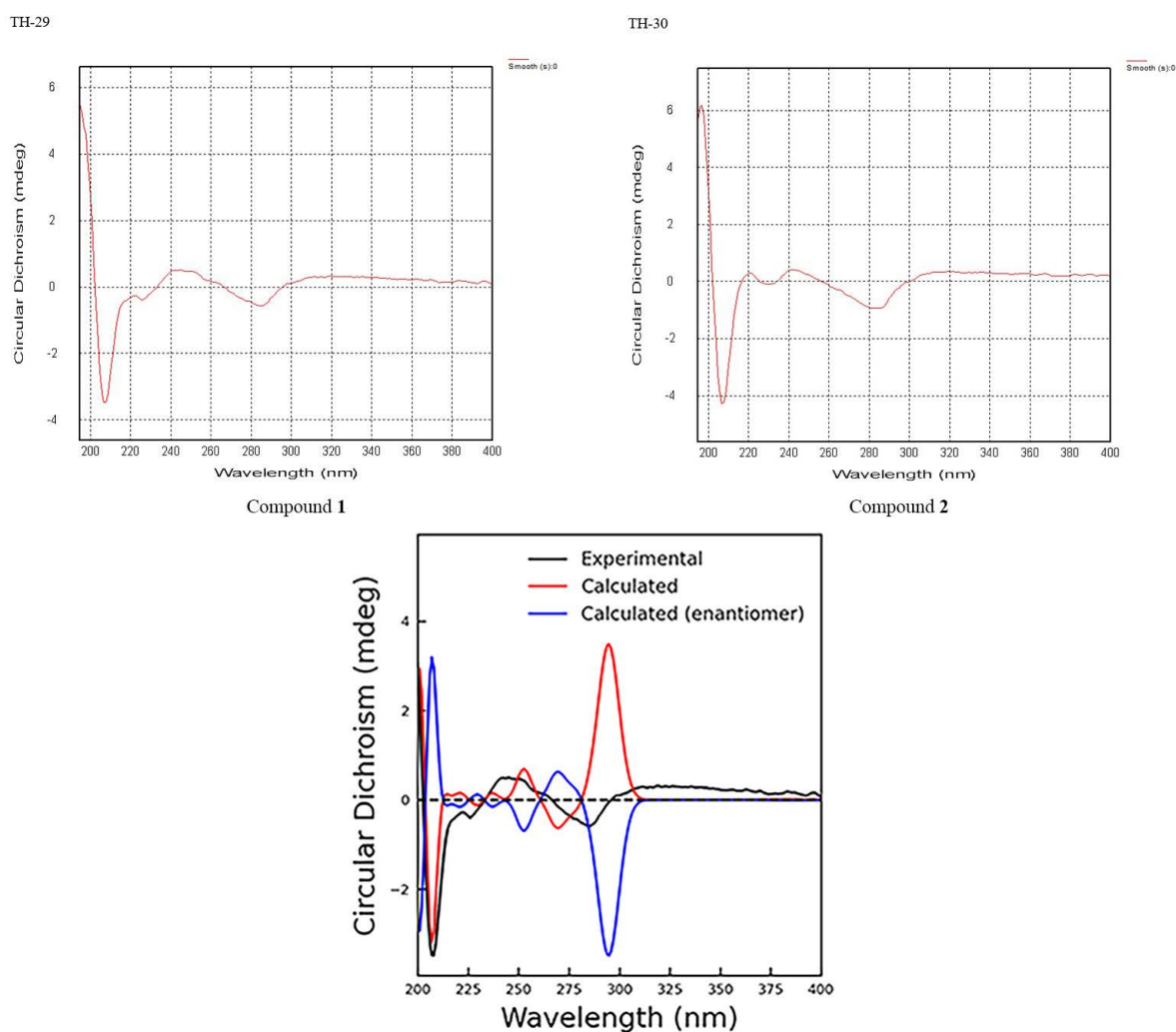


Figure 3. The CD and ECD spectra of compounds 1–2.

Compound 2 was obtained as a colorless amorphous solid. HR-ESI-MS analysis revealed the molecular formula to be $C_{26}H_{28}O_{11}$ based on the $[M + Na]^+$ signal at m/z : 539.1525 (calculated value of 539.1524 $[M + Na]^+$) with the calculated unsaturation (Ω) = 13. The 1H -NMR (Table 1) spectrum of compound 2 exhibited two aromatic ring proton signals δ_H 7.61 (2H, *dd*, J = 1.9, 7.8 Hz, H-2''', H-6'''); 7.42 (3H, *m*, H-3''', H-4''', H-5'''); δ_H 6.23 (1H, *d*, J = 2.9 Hz, H-3'); 6.18 (1H, *d*, J = 2.9 Hz, H-5'); a double bond signal δ_H 7.73 (1H, *d*, J = 16.0 Hz, H-7'''); 6.54 (1H, *d*, J = 16.0 Hz, H-8''') identified as *trans* by the coupling constant, together with one anomeric proton δ_H 4.57 (1H, *d*, J = 7.6 Hz, H-1''). The ^{13}C -NMR spectrum data (Table 1) showed two benzene ring carbons and one pair of olefin carbons δ_C 103.4, 109.2, 118.5, 129.4, 130.1, 131.6, 132.9, 135.7, 138.6, 146.8, 151.6, 155.9; two ester carbonyl data δ_C 168.3, 180.4; and one sugar unit data δ_C 64.7, 71.5, 75.4, 76.0, 77.9, 107.6; and the remaining four carbons were identified by DEPT135° as three methylene δ_C 28.3, 29.5, 82.8 and one hypomethyl δ_C 36.6. Thus, the skeleton was identified as a five-membered lactone ring fragment by the key 1H - 1H COSY signal (Figure 1). Through a data comparison, compound 2 was similar to compound 1 and was determined to contain a cinnamoyl fragment, a sugar fragment, and an aromatic ring fragment, differing in the five-membered lactone ring portion. The connection mode of each segment was determined by key HMBC signals (Figure 1) including H₂-3 and H₁-5 to C-2; H₂-6 to C-4, C-1', C-5' and C-6'; H₁-6'' to C-5'', C-4'' and C-9'''; H₁-8''' to C-9'''; H₁-7''' to C-2''', and C-9'''.

compounds **2** (Figures S12–S21) were available as Supporting Information. The structure is shown in Figure 2. The structure of compound **2** was similar to that of Myrsinoside A [21].

The conformation of the sugar was inferred to be β -D-glucose based on $^1\text{H-NMR}$ and $^{13}\text{C-NMR}$ by comparison with the known literature, and the acid hydrolysis of glucose confirmed that the sugar contained in compound **2** was D-glucose, and the relative conformation of the sugar was determined to be β due to the $\text{H}_2\text{-}1''$ coupling constant of 7.6 Hz, so it was β -D-glucose. By comparing the 1D and 2D NMR spectra, the absolute configuration of compound **2** at the 5-position was the same as that of compound **1**, which was confirmed by CD spectroscopy, so the structure of compound **2** was characterized as ((2R,3S,4S,5R,6S)-6-(2,4-dihydroxy-6-(((S)-5-oxotetrahydrofuran-2-yl) methyl) phenoxy)-3,4,5-trihydroxytetrahydro-2H-pyran-2-yl) methyl (E)-3-phenylacrylate and named as Ardisicreolide B.

The known compounds (**3–6**) were identified on the basis of a detailed spectroscopic interpretation in comparison to the reported data in the references, to be Quercetin (**3**) [22], Myricetrin (**4**) [23], Quercitrin (**5**) [24], and Tamarixetin 3-O-rhamnoside (**6**) [25] (Figure 1). Their $^1\text{H-NMR}$ (400 MHz) and $^{13}\text{C-NMR}$ (100 MHz) data were in the supporting information (Tables S4 and S5).

2.2. Effect of Compounds 1–6 on Antibacterial Activities

The inhibitory activities of compounds **1–6** were determined by measuring the diameter of the inhibition zone against six bacteria (*Escherichia coli*, *Bacillus subtilis*, *Staphylococcus aureus*, *Enterococcus faecalis*, *Pseudomonas aeruginosa*, and *Pseudomonas aeruginosa*) with 50 $\mu\text{g/mL}$ ceftiofur sodium (Cef) as a positive control. The results showed that Ardisicreolide B had a better inhibition effect on *Bacillus subtilis* (Table 2).

Table 2. The antibacterial activities of Ardisicreolide B. (mean \pm SD, $n = 3$) (d, mm).

C($\mu\text{g/mL}$)	Ardisicreolide B			Cef ^a
	25	50	100	
<i>Escherichia coli</i>	-	-	-	16.63 \pm 0.99
<i>P. aeruginosa</i>	-	-	-	19.30 \pm 1.42
<i>Bacillus subtilis</i>	11.33 \pm 1.01	13.2 \pm 1.01	17.47 \pm 1.53	29.37 \pm 1.01
<i>Enterococcus Faecalis</i>	-	-	-	19.40 \pm 1.01
<i>Proteus vulgaris</i>	-	-	-	18.47 \pm 0.78
<i>Staphylococcus aureus</i>	-	-	-	28.40 \pm 1.35

^a Positive control.

2.3. Effects of Compounds 1–2 on RAW264.7 Cells by CCK-8 Method

To find anti-inflammatory compounds, the effect of Ardisicreolides A and B on the cell viability of LPS-stimulated RAW264.7 cells was evaluated with the cck-8 reagent. LPS activation of RAW264.7 cells could result in enhanced activity, and positive drug and compounds **1–6** were compared with the LPS-stimulated group alone. It was found that Ardisicreolide A had significant anti-inflammatory activity at $\geq 20 \mu\text{M/mL}$, and Ardisicreolide B at $\geq 40 \mu\text{M/mL}$ showed significant anti-inflammatory activity (Table 3). Therefore, Ardisicreolides A and B were tentatively identified as compounds with potential anti-inflammatory activity (Figure 4), IC_{50} see Table 3.

Table 3. The IC_{50} values of Ardisicreolides A and B as inhibitors of LPS-treated RAW264.7 cells.

Compound	Mean \pm SD ($\mu\text{M/mL}$)
Ardisicreolide A	24.46 \pm 1.57
Ardisicreolide B	55.85 \pm 4.28

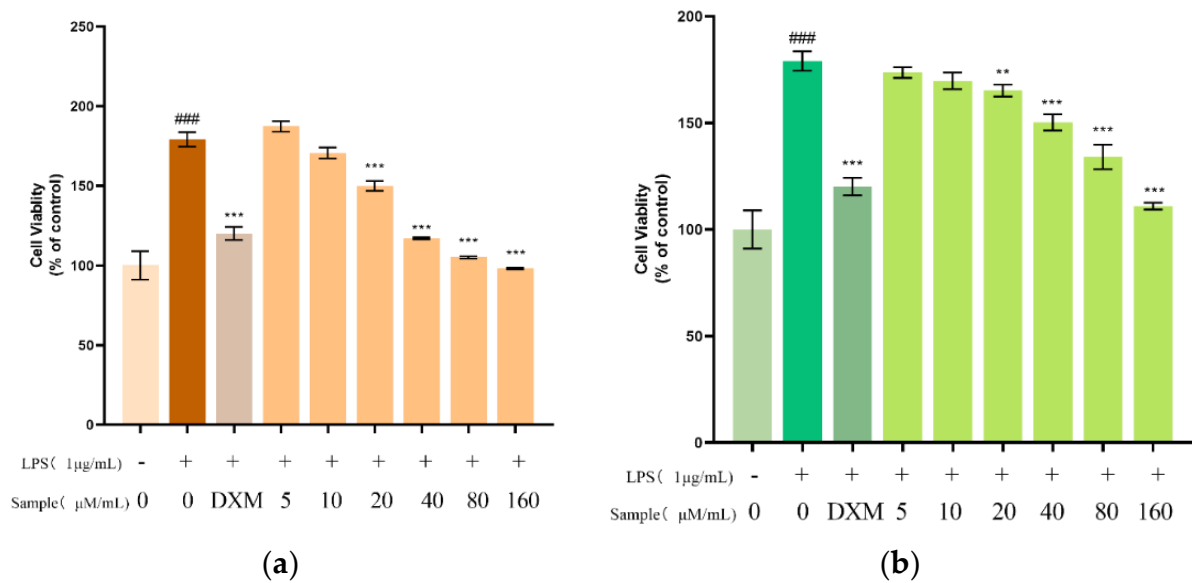


Figure 4. The effects of Ardisicreolides A (a) and B (b) on the cell viability of LPS-treated RAW264.7 cells. The data were expressed as the mean \pm SD ($n = 3$). ** $p < 0.01$, *** $p < 0.001$ versus the control cells that were treated with LPS. ### $p < 0.001$ versus the control group.

2.4. Effects of Compounds 1–2 on NO Production

NO has a variety of regulatory effects on inflammation, and plays an increasingly important role in mediating inflammatory response. Therefore, Griess reagents were used to measure the effect of Ardisicreolides A and B on NO production in LPS-stimulated RAW264.7 cells, and dexamethasone was used as a positive control to evaluate the anti-inflammatory activity of the compounds. As a result (Table S6 in supporting information), both Ardisicreolides A and B showed inhibitory activity on the amount of NO release (Figure 5), however, the activity could not correlate significantly with the compound concentration.

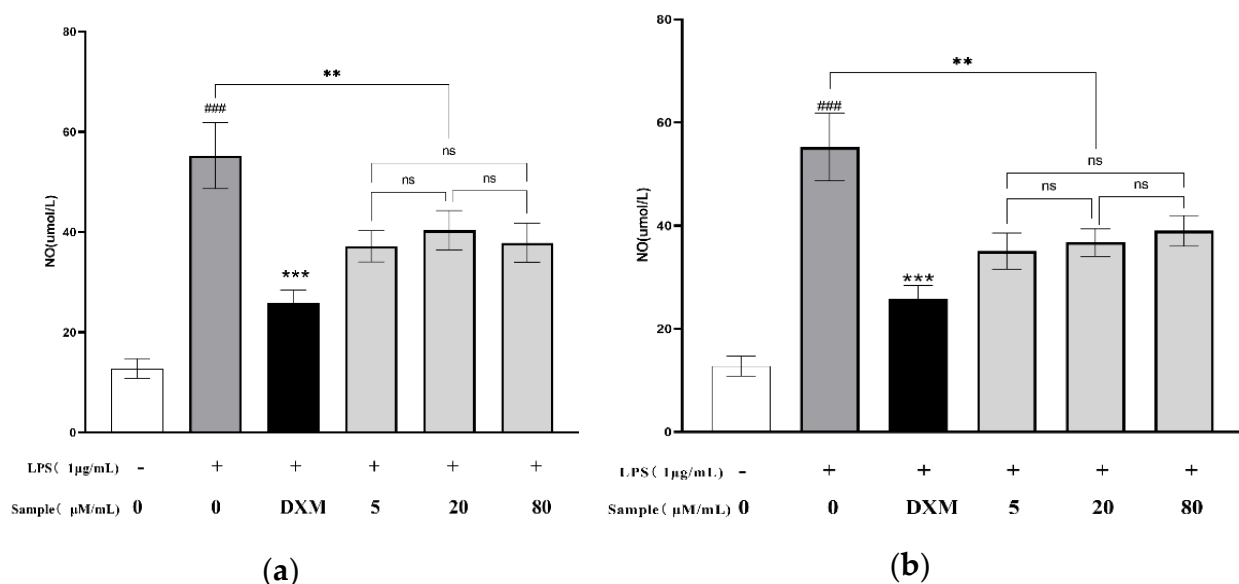


Figure 5. Ardisicreolides A (a) and B (b) decreased NO production. Dexamethasone with 1 µg/mL was used as the positive control. The data were expressed as the mean \pm SD ($n = 3$). ns > 0.05 , ** $p < 0.01$, *** $p < 0.001$ versus the model cells that were treated by LPS. ### $p < 0.001$ versus the control.

2.5. Effects of Compounds 1–2 on Inflammatory Cytokines Production

IL-1 β , IL-4, IL-10, and TNF- α are important inflammatory regulators produced in the process of inflammatory response. They can be produced and released in large amounts under the conditions of infection, injury, and immune response [26]. Therefore, they are commonly used as indicators to assess the anti-inflammatory effects of natural compounds [27,28]. In this paper, the effects of new compounds on the production of IL-1 β , IL-4, IL-10, and TNF- α release by LPS-stimulated RAW264.7 cells were quantified with ELISA kits. As shown in Figure 6 (Table S7 in supporting information), Ardisicreolides A and B had significant effects on IL-1 β , IL-4, IL-10, and TNF- α at $\geq 5 \mu\text{M}/\text{mL}$. This indicates that both Ardisicreolides A and B could effectively inhibit the inflammatory response of the LPS-stimulated RAW264.7 cells (Figure 6).

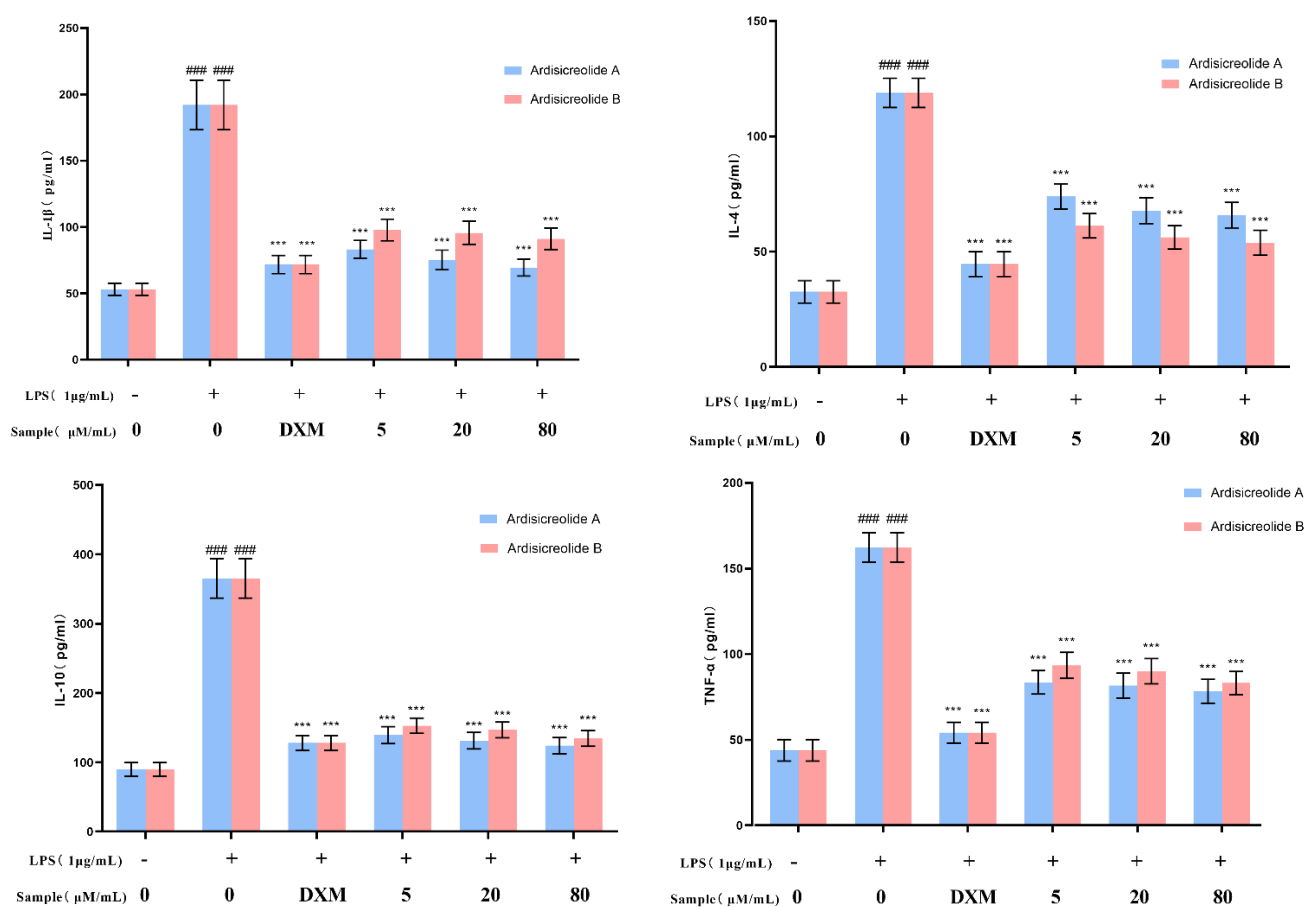


Figure 6. Ardisicreolides A and B decreased the inflammatory cytokine production. Dexamethasone with 40 $\mu\text{g}/\text{mL}$ was used as the positive control. The data were expressed as the mean \pm SD ($n = 3$). *** $p < 0.001$ compared to the model cells that were treated by LPS. #### $p < 0.001$ versus the control.

3. Materials and Methods

3.1. General Experimental Procedures

The 1D and 2D NMR spectra were recorded on a Bruker DPX 400 instrument (Bruker, Bremen, Germany) with tetramethylsilane as the internal standard and MeOH- d_4 as the solvent. The HR-ESI-MS experiments were performed on a Waters Xevo G2-S QTOF (Waters Corporation, Milford, MA, USA). The semi-preparative HPLC procedure was performed on a Shimadzu LC-16P instrument with a RID-20A (Shimadzu Tokyo, Japan) and a reversed-phase C18 column (250 \times 10 mm, 5 μm , Shim-pack GIST, Shimadzu Tokyo, Japan). UV spectra were scanned with a SHIMADZU UV-2401PC spectrometer (Shimadzu Tokyo, Japan). Infrared spectra were performed on a VERTEX 70 spectrometer (Bruker, Bremen, Germany) using KBr particles. The rotational luminosity was measured on an

Autopol VI instrument. Electron circular dichroism spectra were recorded on a LAAPD detector. Column chromatography was performed with silica gel (200–300 mesh, Qingdao Marine Chemical Ltd., Qingdao, China) and octadecyl silica gel (ODS) (50 μm , Merck, Darmstadt, Germany).

3.2. Plant Material

The leaves of *Ardisia crenata* Sims were collected from Guiyang in Guizhou Province (China), and identified by Professor Sheng-hua Wei from Guizhou University of Traditional Chinese Medicine. The voucher specimen (Accession number: 20200908) was deposited at the Guizhou University of Traditional Chinese Medicine.

3.3. Extraction and Isolation

The dried leaves (5 kg) of *Ardisia crenata* Sims were crushed, extracted with 70% ethanol at reflux for three times, the solvent was recovered under reduced pressure to obtain the crude extract, and the suspension was obtained by adding 10 L of distilled water. The crude extract was partitioned with petroleum ether, EtOAc, and n-BuOH successively to yield EtOAc (522.0 g) extracts. The soluble fraction of the EtOAc (220.8 g) was eluted by dichloromethane-methanol (0:1–1:0) on a silica gel column for a total of ten fractions (Fr. A–J). Fraction D (5.0 g) was chromatographed on an ODS column with MeOH-H₂O (1:9 to 1:0) to afford sub-fractions D1–D9, Fr. D5 was eluted by MCI with MeOH-H₂O (3:7 to 1:0) to afford sub-fractions D51–D58 and Fr. D55 was separated by semi-preparative HPLC (MeOH-H₂O, 62:38; flow rate: 3 mL·min^{−1}) to obtain compound 1 (5.9 mg t_R = 13.7 min), compound 2 (3.6 mg t_R = 19.5 min), and compound 5 (9.0 mg t_R = 21.4 min). Fraction E (9.6 g) was chromatographed on an ODS column with MeOH-H₂O (1:9 to 1:0) to afford sub-fractions E1–E9, Fr. E4 was separated by semi-preparative HPLC (MeOH-H₂O, 55:45; flow rate: 3 mL·min^{−1}) to obtain compound 6 (6.8 mg t_R = 15.0 min). Fraction I (17.6 g) was chromatographed on an ODS column with MeOH-H₂O (1:9 to 1:0) to afford sub-fractions I1–I9, Fr. I4 was separated by semi-preparative HPLC (MeOH-H₂O, 45:55; flow rate: 3 mL·min^{−1}) to obtain compound 3 (7.2 mg t_R = 20.0 min) and compound 4 (6.8 mg t_R = 34.2 min).

3.4. Characterization of Compounds 1–2

Ardisicreolide A, Yellowish amorphous solid; $[\alpha]_D^{24} + 14.23$ (c 0.05, MeOH); UV (MeOH) λ (log ϵ) 203 (4.29) nm; HR-ESI-MS m/z 539.1522 [M + Na]⁺ (Calcd for C₂₆H₂₈O₁₁, 539.1524); ¹H and ¹³C NMR data (CD₃OD), see Table 1.

Ardisicreolide B, Colorless amorphous solid; $[\alpha]_D^{24} - 22.65$ (c 0.08, MeOH); UV (MeOH) λ (log ϵ) 203 (4.45) nm; HR-ESI-MS m/z 539.1525 [M + Na]⁺ (Calcd for C₂₆H₂₈O₁₁, 539.1524); ¹H and ¹³C NMR data (CD₃OD) see Table 1.

3.5. Antibacterial Activity Screening

The blank drug sensitive test paper was dipped to 50 $\mu\text{g}/\text{mL}$ of ceftiofur sodium solution and the compound solution of each concentration, respectively. A total of 100 μL of the test solutions (*Escherichia coli*, *P. aeruginosa*, *Enterococcus faecalis*, *Proteus vulgaris*, *Staphylococcus aureus*, and *Bacillus subtilis*) were absorbed respectively, and LB medium was spread evenly using a sterile applicator stick, and took the drug-sensitive test paper with sterile forceps and spread it evenly on the center of the surface of the medium in the divided area correspondingly. Then, the medium was put in a constant temperature incubator until the drug solution adsorbed into the medium, and was incubated at 37 °C for 8 h, and measured the diameter of the inhibition zone by repeating it three times and recording the data.

3.6. Cell Culture

The RAW264.7 cell lines were obtained from the Chinese Academy of Sciences (Shanghai, China) cell bank and cultured in DMEM supplemented with 10% (*v/v*) heat-inactivated

FBS at 37 °C in a fully humidified incubator containing 5% CO₂. The cells were passaged when they grew to 80–90% confluence.

3.7. Primary Screening for Anti-Inflammatory Compounds

The RAW264.7 cells were inoculated in complete medium containing double antibiotics in 10% FBS at 37 °C with 5% CO₂ in a constant temperature incubator, and 96-well plates were inoculated with cell suspensions (100 uL/well) at a density of 10⁵/mL at 37 °C with 5% CO₂ in a constant temperature incubator. Then, cells were pretreated with different isolated compounds (5–160 µM) or dexamethasone (40 µg/mL) for 1 h and then stimulated with LPS (1 µg/mL). The normal and model cells were stimulated with or without 1 µg/mL LPS for 24 h. All samples were tested in quadruplicate according to the CCK-8 kit after incubation.

3.8. Determination of Inflammatory Cytokines

The RAW264.7 cells were plated in 24-well plates and incubated at 37 °C and 5% CO₂ for 24 h. Then, cells were pretreated with different isolated compounds (5, 20, 80 µM) or dexamethasone (40 µg/mL) for 1 h and then stimulated with LPS (1 µg/mL). The normal and model cells were stimulated with or without 1 µg/mL LPS for 24 h. The supernatants of the RAW264.7 cells after drug administration and culture were used to determine the NO release according to the Griess method, and the contents of IL-1β, IL-4, IL-10, and TNF-α in the cells were determined according to enzyme-linked immunosorbent assay kits (ELISA) following the manufacturer's instructions [29], and all samples were taken in triplicate.

4. Conclusions

In summary, a total of six compounds were isolated and identified from the EtOAc fraction of the 70% ethanol extract of the leaves of *Ardisia crenata* Sims including two new lactone structures Ardisicreolides A and B, which were analyzed and identified mainly by MS, NMR, and IR. In previous studies, *A. crenata* Sims components focused on triterpene saponins, isocoumarins, and benzoquinones, however, lactones were rarely identified. In this paper, we evaluated the antibacterial and anti-inflammatory activities of two new lactones isolated and identified, in which Ardisicreolide B showed good inhibition of *Bacillus subtilis* at ≥50 µg/mL (IZD = 13.2 ± 1.01 mm), and both Ardisicreolides A and B exhibited significant anti-inflammatory activity against inflammatory factors of NO, IL-1β, IL-4, IL-10 and TNF-α release with varying degrees. Therefore, the lactone components in the leaves of *A. crenata* Sims might be natural effective drugs for anti-inflammatory drug development, and the non-traditional medicinal parts of *A. crenata* Sims could be identified as a source of natural anti-inflammatory molecules, which is of great significance for the rational development and application of *A. crenata* Sims.

Supplementary Materials: The following supporting information can be downloaded at: <https://www.mdpi.com/article/10.3390/molecules27154903/s1>, Figure S1: Chemical structure of compounds 1; Figures S2–S21: the spectroscopic data for compounds 1–2; Table S1: Energies of configurations 1; Table S2: Energies of configurations 1 at B3LYP/6-311G(d,p) in methanol; Table S3: Standard orientations of configurations 1 for ECD calculation; Table S4: ¹³C-NMR and ¹H-NMR Data of 3–4 in CD₃OD; Table S5: ¹³C-NMR and ¹H-NMR Data of 5–6 in CD₃OD; Table S6: Effects of Ardisicreolides A and B on NO release of raw cells; Table S7: The effects of Ardisicreolides A and B on production release of TNF-α, IL-1β, IL-4 and IL-10.

Author Contributions: Y.Z. (Ying Zhou) and Y.Z. (Yongqiang Zhou) designed the experiments. H.T., X.Y. and X.W. performed the data analysis. H.T. isolated and purified the compounds. H.T. and Y.Z. (Yongqiang Zhou) wrote the article, while critical revision of the publication was performed by all authors. All authors have read and agreed to the published version of the manuscript.

Funding: The project was supported by the National Key R&D Program of China (No. 2018YFC1708100); the Science and Technology Plan Project of Guizhou (Qian Ke He Pingtai Rencai [2019]5407); and the Special project of scientific research and innovation exploration of Guizhou University of Traditional Chinese Medicine (No. 2018YFC170810102).

Institutional Review Board Statement: Not applicable.

Informed Consent Statement: Not applicable.

Data Availability Statement: Not applicable.

Conflicts of Interest: The authors declare no conflict of interest.

Sample Availability: Samples of all of the isolated compounds are available from the authors.

References

1. Kobayashi, H.; De Mejía, E. The genus *Ardisia*: A novel source of health-promoting compounds and phytopharmaceuticals. *J. Ethnopharmacol.* **2005**, *96*, 347–354. [[CrossRef](#)] [[PubMed](#)]
2. Anh, N.H.; Ripperger, H.; Schmidt, J.; Porzel, A.; Van Sung, T.; Adam, G. Resorcinol derivatives from two *Ardisia* species. *Planta Med.* **1996**, *62*, 479–480. [[CrossRef](#)]
3. Zaima, K.; Deguchi, J.; Matsuno, Y.; Kaneda, T.; Hirasawa, Y.; Morita, H. Vasorelaxant effect of FR900359 from *Ardisia crenata* on rat aortic artery. *J. Nat. Med.* **2012**, *67*, 196–201. [[CrossRef](#)] [[PubMed](#)]
4. Liu, D.L.; Wang, N.L.; Zhang, X.; Gao, H.; Yao, X.S. Two new triterpenoid saponins from *Ardisia crenata*. *J. Asian Nat. Prod. Res.* **2007**, *9*, 119–127. [[CrossRef](#)] [[PubMed](#)]
5. Liu, D.L.; Wang, N.L.; Zhang, X.; Yao, X.S. Three new triterpenoid saponins from *Ardisia crenata*. *Helv. Chim. Acta* **2011**, *94*, 693–702. [[CrossRef](#)]
6. Li, M.; Wei, S.-Y.; Xu, B.; Guo, W.; Liu, D.-L.; Cui, J.-R.; Yao, X.-S. Pro-apoptotic and microtubule-disassembly effects of ardisiacrispin (A + B), triterpenoid saponins from *Ardisia crenata* on human hepatoma Bel-7402 cells. *J. Asian Nat. Prod. Res.* **2008**, *10*, 729–736. [[CrossRef](#)] [[PubMed](#)]
7. Zheng, Z.-F.; Xu, J.-F.; Feng, Z.-M.; Zhang, P.-C. Cytotoxic triterpenoid saponins from the roots of *Ardisia crenata*. *J. Asian Nat. Prod. Res.* **2008**, *10*, 833–839. [[CrossRef](#)]
8. Ma, L.; Li, W.; Wang, H.; Kuang, X.; Li, Q.; Wang, Y.; Xie, P.; Koike, K. A simple and rapid method to identify and quantitatively analyze triterpenoid saponins in *Ardisia crenata* using ultrafast liquid chromatography coupled with electrospray ionization quadrupole mass spectrometry. *J. Pharm. Biomed. Anal.* **2015**, *102*, 400–408. [[CrossRef](#)]
9. Ning-Ning, S.; Lei-Min, Y.; Zhang, M.-J.; Ren-Feng, A.; Wei, L.; Huang, X.-F. Triterpenoid saponins and phenylpropanoid glycoside from the roots of *Ardisia crenata* and their cytotoxic activities. *Chin. J. Nat. Med.* **2021**, *19*, 63–69.
10. Sun, X.; Yao, C.; FU, S.; Gong, Z.; Liu, T.; Yang, C.; Zha, J.; LI, Y. Study on HPLC Fingerprint of Miao Medicine *Ardisia crenata*. *China Pharm.* **2017**, *28*, 4285–4288.
11. Jain, P.K.; Joshi, H. Coumarin: Chemical and pharmacological profile. *J. Appl. Pharm. Sci.* **2012**, *2*, 236–240.
12. Qin, H.-L.; Zhang, Z.-W.; Ravindar, L.; Rakesh, K. Antibacterial activities with the structure-activity relationship of coumarin derivatives. *Eur. J. Med. Chem.* **2020**, *207*, 112832. [[CrossRef](#)]
13. Yu, J.-H.; Yu, Z.-P.; Wang, Y.-Y.; Bao, J.; Zhu, K.-K.; Yuan, T.; Zhang, H. Triterpenoids and triterpenoid saponins from *Dipsacus asper* and their cytotoxic and antibacterial activities. *Phytochemistry* **2019**, *162*, 241–249. [[CrossRef](#)] [[PubMed](#)]
14. Wang, Z.; Jiang, M.; Khan, A.; Cai, S.; Li, X.; Liu, J.; Kai, G.; Zhao, T.; Cheng, G.; Cao, J. Epigynumgenane-type pregnane glycosides from *Epigynum cochinchinensis* and their immunosuppressive activity. *Phytochemistry* **2019**, *168*, 112127. [[CrossRef](#)]
15. Gao, F.; Yao, Y.-C.; Cai, S.-B.; Zhao, T.-R.; Yang, X.-Y.; Fan, J.; Li, X.-N.; Cao, J.-X.; Cheng, G.-G. Novel immunosuppressive pregnane glycosides from the leaves of *Epigynum auritum*. *Fitoterapia* **2017**, *118*, 107–111. [[CrossRef](#)] [[PubMed](#)]
16. Jin, H.-G.; Kim, K.-W.; Li, J.; Lee, D.Y.; Yoon, D.; Jeong, J.T.; Kim, G.-S.; Oh, H.; An, R.-B.; Kim, Y.-C. Anti-inflammatory components isolated from *Atractylodes macrocephala* in LPS-induced RAW264. 7 macrophages and BV2 microglial cells. *Appl. Biol. Chem.* **2022**, *65*, 1–13. [[CrossRef](#)]
17. Paço, A.; Brás, T.; Santos, J.O.; Sampaio, P.; Gomes, A.C.; Duarte, M.F. Anti-Inflammatory and Immunoregulatory Action of Sesquiterpene Lactones. *Molecules* **2022**, *27*, 1142. [[CrossRef](#)]
18. Wang, J.-C.; Shi, Q.; Zhou, Q.; Zhang, L.-L.; Qiu, Y.-P.; Lou, D.-Y.; Zhou, L.-Q.; Yang, B.; He, Q.-J.; Weng, Q.-J. Sapidolide A alleviates acetaminophen-induced acute liver injury by inhibiting NLRP3 inflammasome activation in macrophages. *Acta Pharmacol. Sin.* **2022**, 1–10. [[CrossRef](#)]
19. Robinson, S.L.; Christenson, J.K.; Wackett, L.P. Biosynthesis and chemical diversity of β -lactone natural products. *Nat. Prod. Rep.* **2019**, *36*, 458–475. [[CrossRef](#)]
20. Silva, R.; Coelho, E.; Aguiar, T.Q.; Domingues, L. Microbial biosynthesis of lactones: Gaps and opportunities towards sustainable production. *Appl. Sci.* **2021**, *11*, 8500. [[CrossRef](#)]
21. Zou, Y.P.; Tan, C.H.; Wang, B.D.; Zhu, D.Y.; Kim, S.K. Chemical constituents from *Myrsine africana* L. *Helv. Chim. Acta* **2008**, *91*, 2168–2173. [[CrossRef](#)]

22. Li, Y.; Wu, M.; Dong, H.; Yu, P.; Lu, L.; Du, W.; Cao, S. Total Synthesis and Anti-Inflammatory Activity of Velutone F. *Nat. Prod. Commun.* **2022**, *17*, 1934578X221076653. [[CrossRef](#)]
23. Wang, W.; Wu, Y.; Li, C.; Yang, Y.; Li, X.; Li, H.; Chen, L. Synthesis of New Lathyrane Diterpenoid Derivatives from *Euphorbia lathyris* and Evaluation of Their Anti-Inflammatory Activities. *Chem. Biodivers.* **2020**, *17*, e1900531. [[CrossRef](#)]
24. Nemeth, E.; Rivera, S.; Gabayan, V.; Keller, C.; Taudorf, S.; Pedersen, B.K.; Ganz, T. IL-6 mediates hypoferremia of inflammation by inducing the synthesis of the iron regulatory hormone hepcidin. *J. Clin. Investig.* **2004**, *113*, 1271–1276. [[CrossRef](#)] [[PubMed](#)]
25. Nathan, C.; Xie, Q.-W. Nitric oxide synthases: Roles, tolls, and controls. *Cell* **1994**, *78*, 915–918. [[CrossRef](#)]
26. Li, L.-C.; Ning, D.-S.; Fu, Y.-X.; Pan, Z.-H. Structure elucidation and anti-inflammatory mechanism of difengpienol C, a new neolignan isolated from *Illicium difengpi*. *Fitoterapia* **2021**, *153*, 104949. [[CrossRef](#)]
27. Zheng, Y.; Tian, C.; Fan, C.; Xu, N.; Xiao, J.; Zhao, X.; Lu, Z.; Cao, H.; Liu, J.; Yu, L. Sheng-Mai Yin exerts anti-inflammatory effects on RAW 264.7 cells and zebrafish. *J. Ethnopharmacol.* **2021**, *267*, 113497. [[CrossRef](#)]
28. Kim, T.-W.; Shin, J.-S.; Chung, K.-S.; Lee, Y.-G.; Baek, N.-I.; Lee, K.-T. Anti-Inflammatory mechanisms of Koreanaside A, a lignan isolated from the flower of *Forsythia koreana*, against LPS-induced macrophage activation and DSS-induced colitis mice: The crucial role of AP-1, NF- κ B, and JAK/STAT signaling. *Cells* **2019**, *8*, 1163. [[CrossRef](#)]
29. Li, M.; Li, B.; Hou, Y.; Tian, Y.; Chen, L.; Liu, S.; Zhang, N.; Dong, J. Anti-inflammatory effects of chemical components from *Ginkgo biloba* L. male flowers on lipopolysaccharide-stimulated RAW264. 7 macrophages. *Phytother. Res.* **2019**, *33*, 989–997. [[CrossRef](#)]